Forward Physics at RHIC with BRAHMS

K. Hagel[1]

(for The BRAHMS collaboration)

[1] *Cyclotron Institute, Texas A&M University, College Station, Texas 77843**

(Dated: December 16, 2004)

A summary of BRAHMS results is presented. Emphasis is placed on data for which measurements at forward rapidities are necessary for interpretation. This includes measurements of spectra over a wide range of y and transverse momentum, yields, stopping, quark chemistry and high p_t suppression in both Au+Au and d+Au collisions at $\sqrt{s_{NN}} = 200$ GeV.

PACS numbers: 25.70.Pq, 24.60.Ky, 05.70.Jk
Keywords: Quark Chemistry, Rapidity Density, Stopping, High p_t suppression

INTRODUCTION

Detailed measurements over a wide region of phase space are very important in understanding possible new states of matter at RHIC energies where $\sqrt{s_{NN}} = 200$ GeV. BRAHMS has the unique capability of providing detailed high resolution information from mid-rapidity to a rapidity as high as 4.

In this contribution we summarize the results of various measurements over a large region of phase space using BRAHMS. We focus on the measurements where the particular characteristics of BRAHMS can be exploited to obtain unique information. These measurements include quark chemistry over a large range of rapidity where we can learn about properties of hot dense matter. We show a breakdown of "Boost Invariance" for $y >\sim 1$ which favors a description more in line with Landau Hydrodynamics. A summary of our study of stopping gives us information on the energy loss of participants in Au+Au collisions. Finally, high p_t suppression studies in Au+Au and d+Au give both information on the observation of a hot dense system and on the initial conditions of Au nuclei before collisions.

All of the measurements presented are derived from the identified particle spectra for $0 < y < 3.2$ which, after suitable fitting, lead to the measured yields. Unless otherwise noted, the data shown are from the 5% most central collisions. A description of the setup can be found in [1].

SPECTRA AND YIELDS

Spectra of positive and negative pions, kaons and protons were collected and analyzed. The negative particle π, K and p spectra are shown in figure 1. We note that the shapes of the spectra are different for the different species. The different spectra were fit with different functions in transverse momentum, p_t or transverse mass, $m_t = \sqrt{p_t^2 + m^2}$, depending on the shape of the spectrum of a given particle. The pion spectra were fit with a power law, $(1 + \frac{p_t}{p_0})^{-n}$, the kaon spectra with an exponential, $\exp(\frac{m_t - m}{T})$ and the proton spectra with a Gaussian, $\exp(-\frac{p_t^2}{2\sigma^2})$. The dashed lines in figure 1 show the fits to the various spectra.

From the fits one can extract the yields by integrating the appropriate functions over the entire m_t range. This gives the rapidity densities shown in the upper panel of figure 2. The positive and negative pions show nearly the same distribution over the entire rapidity range measured while the anti-protons show a decrease as the rapidity approaches the beam rapidity. There is also an increasing production of K^+ over K^- as the forward rapidity region is approached. The lower panel shows the average transverse momenta of the identified particles. There is no significant difference between the particles and their anti-particles.

QUARK CHEMISTRY

Anti-particle to particle ratios can yield important information on the dynamics of reaction mechanisms in large systems [2, 3]. In figure 3 we show such anti-particle to particle ratios [4] for the π, K and p as a function of rapidity for the top 20% central collisions. We see, as noted above, that the pion ratios remain close to unity over the entire rapidity range measured. The K^-/K^+ ratios, however, show a decrease from 0.95 ± 0.05 near mid-rapidity to 0.67 ± 0.06 at $y \sim 3$. The K^-/K^+ and $\bar{p}/p$ ratios are roughly constant in the interval of $0 < y < 1$. The $\bar{p}/p$ ratios, nearly constant at about 0.75 for $y < 1$, show a decrease to about 0.2 at the most forward rapidity studied. The value of $\bar{p}/p \sim 0.75$ at mid-rapidity corresponds to the largest ratio of anti-matter to matter observed to date in the laboratory and indicates that a state of near net-baryon free matter has been created.

The data at mid-rapidity have been analyzed in terms of a thermal model [5] where a proposed parameterization as a function of energy was leads to a prediction for $\sqrt{s_{NN}} = 200$ GeV of T$\sim$ 177 MeV and $\mu_B \sim 30$ MeV. The small value of the baryo-chemical potential

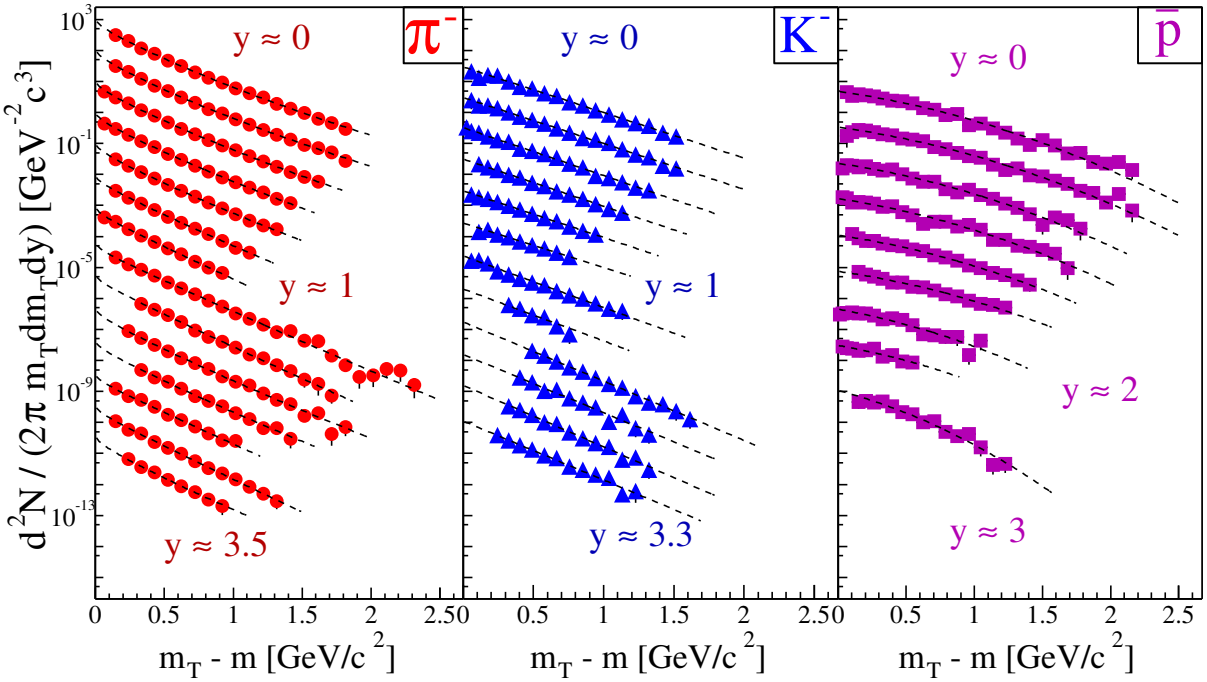

FIG. 1: $m_t - m$ for π^-, K^- and $\bar{p}$ spectra from Au+Au at $\sqrt{s_{NN}} = 200$ GeV at different rapidities. The lines indicate the different fits to the data (see text)

indicates a small net baryon density at mid-rapidity consistent with the fact that the $\bar{p}/p$ ratio is large and close to 1.

A comparison of the K^-/K^+ and $\bar{p}/p$ ratios also shows a remarkable correlation over the entire rapidity range we have measured as seen in figure 4. The figure also shows the results from BRAHMS at $\sqrt{s_{NN}} = 130$ GeV [6] as well as those of similar measurements made at AGS [7] and SPS [8, 9] energies. In a thermal approach where the strange quark chemical potential, μ_s, is fixed by conservation of strangeness [10], the antiparticle to particle ratios are controlled by the light and strange quark fugacities, $\lambda_q = e^{\mu_q/T}$ and $\lambda_s = e^{\mu_s/T}$. This leads to the

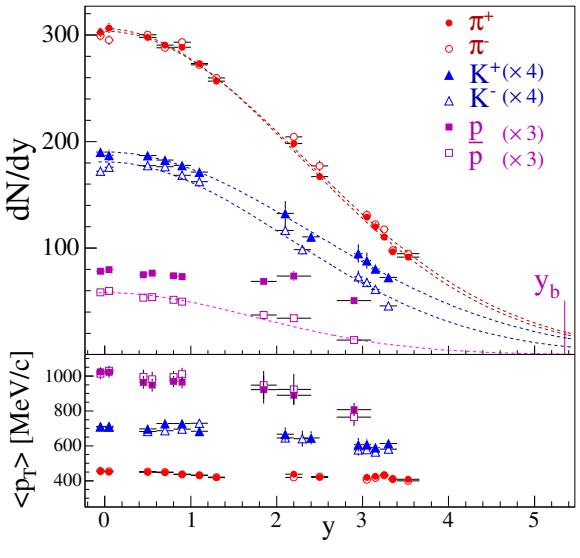

FIG. 2: π, K and p rapidity densities for Au+Au at $\sqrt{s_{NN}} = 200$ GeV (upper panel) and mean transverse momenta $< p_t >$ (lower panel). The yields of produced particles are well described by Gaussian fits.

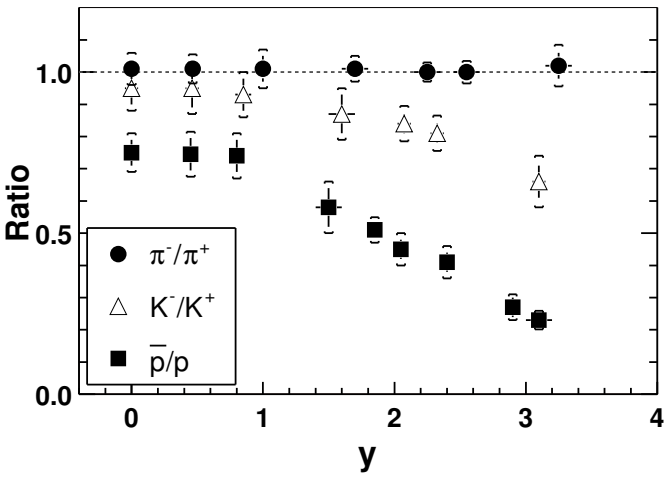

FIG. 3: Anti-hadron to hadron ratios as a function of rapidity in ^{197}Au + ^{197}Au at $\sqrt{s_{NN}} = 200$ GeV for the top 20% central collisions.

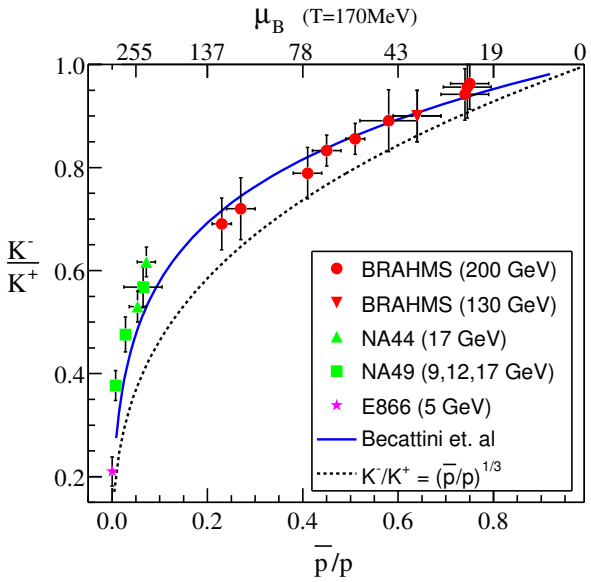

FIG. 4: kaon vs proton ratios. Solid symbols indicate the BRAHMS results in ^{197}Au + ^{197}Au at $\sqrt{s_{NN}}$ and data from reference [6]. The open symbols show lower energy data [7–9]. The line shows the results of Becattini's model [11]. The baryon chemical potential, μ_B shown on the top scale is in MeV.

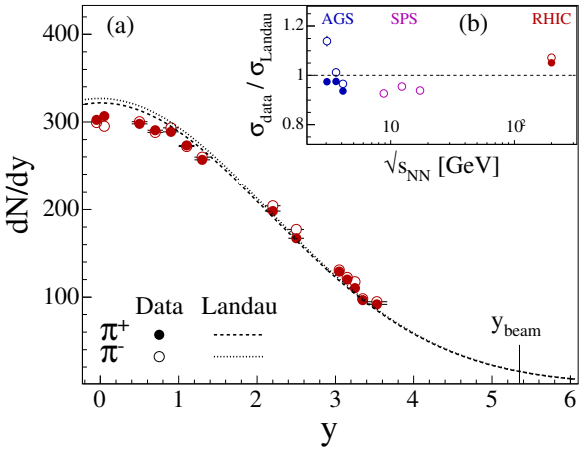

FIG. 5: (a) π dN/dy with a fit to Landau parameters at $\sqrt{s_{NN}}$ = 200 GeV. (b) $\sigma_{N(\pi)}/\sigma_{Landau}$ as a function of $\sqrt{s_{NN}}$

prediction that

$$K^-/K^+ = e^{2\mu_s/T}e^{6\mu_q/T} = e^{2\mu_s/T}(\bar{p}/p)^{\frac{1}{3}} \qquad (1)$$

which reduces to

$$K^-/K^+ = (\bar{p}/p)^{\frac{1}{3}} \qquad (2)$$

for $\mu_s = 0$. This dependence is shown as the dotted line in figure 4. We see that this simple equation slightly underpredicts the data suggesting non-zero strangeness.

The solid line in figure 4 shows the prediction of the grand canonical calculation [11] for a constant temperature of 170 MeV. These results suggest in the context of these models that the baryon chemical potential evolves from about $\mu_B \approx 130$ MeV at $y \sim 3$ to $\mu_B \approx 25$ MeV at mid rapidity.

LANDAU HYDRODYNAMICS

The longitudinal flow in a relativistic heavy ion collision may be sensitive to the initial pressure of the system and possibly the equation of state. Since pions dominate the multiplicities, pion distributions are expected to be a good way to study longitudinal flow. Note that the pion dN/dy in figure 2 is nearly Gaussian. Landau's analytic model of relativistic hydrodynamics in a constant entropy expansion [12] was extended by Carruthers *et al.* [13] to explain rapidity distributions for massless pions in the case where the p_t and rapidity distributions factorize. Under these assumptions the dN/dy of the pions is expected to be Gaussian with a width given by

$$\sigma^2 = \ln\left(\frac{\sqrt{s_{NN}}}{2m_N}\right) \qquad (3)$$

where m_N is the mass of the nucleon.

Figure 5a shows the dN/dy for π^- in Au + Au at $\sqrt{s_{NN}}$ = 200 GeV fitted with a width given by equation 3. We note that the width for the data is slightly broader than the width suggested by Landau Hydrodynamics. The flat region for $y <\sim 1$ may reflect a "boost invariant" picture [14] near mid-rapidity. The inset in figure 5b, shows a compilation of the ratios of the measured widths (from the Gaussian fit to π in figure 2 at $\sqrt{s_{NN}} = 200$ GeV) from AGS to RHIC energies. A difference of about 5% is observed at RHIC and the maximum difference over the large energy range is less than 10%. The logarithmic growth of the width stands in contrast to the linear increase of the multiplicity [15].

NUCLEAR STOPPING

Another measurement which benefits from the unique capabilities of BRAHMS' extensive coverage is that of nuclear stopping. We have deduced the stopping in ^{197}Au + ^{197}Au at $\sqrt{s_{NN}}$ = 200 GeV by measuring the net-proton dN/dy from mid-rapidity to $y \sim 3$ and, from that, estimating the net-baryon dN/dy [16]. The net-baryon dN/dy is shown in figure 6 in the inset. The dashed line shows a fit to the measured data using a Bjorken inspired symmetric sum of 2 Gaussians in momentum space

$$\sum_{\pm} exp\Big[-\frac{(m_N \sinh(y) \pm < p_z >)^2}{2\sigma^2_{p_z}}\Big] \qquad (4)$$

and the solid curve shows a fit to a 6th order polynomial. The fits are constrained by the fact that the total

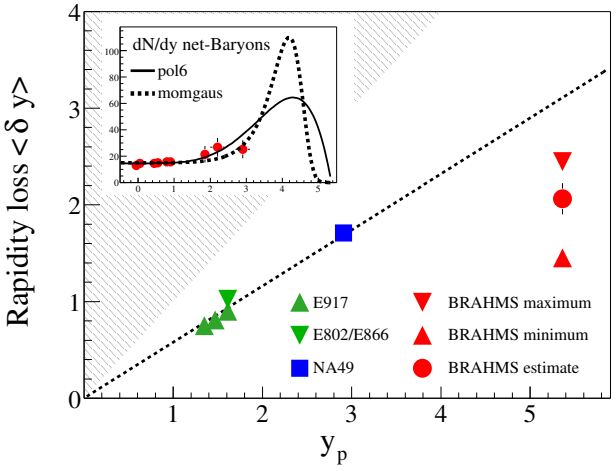

FIG. 6: Rapidity loss using equation 5 as a function of projectile rapidity in the center of mass. The hatched area indicates the unphysical region and the dashed line shows phenomenological scaling $< \delta y >= 0.58 y_p$ extracted from lower energy data [17–19]. Inset: Extrapolated net baryon distribution with different fits to the data (see text)

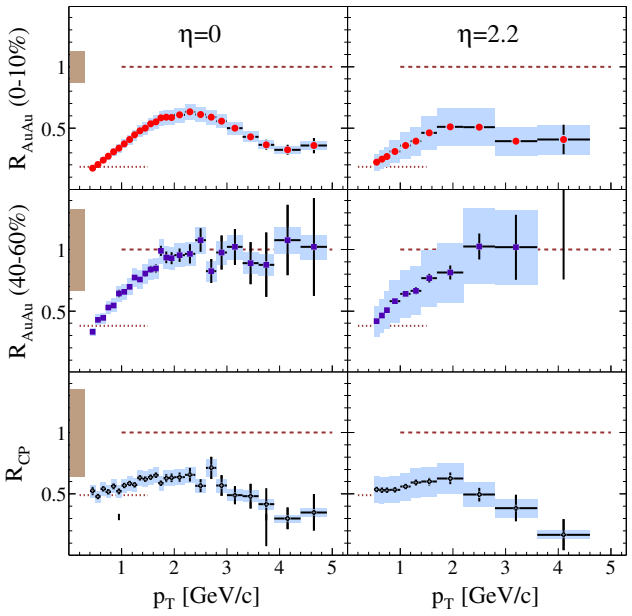

FIG. 7: Top: Nuclear modification factors, R_{AA} as a function of p_t for ^{197}Au + ^{197}Au at $\sqrt{s_{NN}} = 200$ GeV at mid-rapidity (left) and $\eta = 2.2$ (right) for the 0-10% most central collisions. Center: Same as top, but for centrality of 40-60%. Bottom: R_{cp} as a function of p_t.

baryon number, the integral under each curve, must be conserved. From the fits, the rapidity loss can be determined using

$$< \delta y >= y_p - < y >= y_p - \frac{2}{< N_{part} >} \int_0^{y_p} y \frac{dN_{(B-\bar{B})}}{dy} dy \tag{5}$$

where N_{part} is the number of participating nucleons in the collision. The resultant $< \delta y > \approx 2.0$ is shown in figure 6 along with the systematics of data from other energies [17–19]. The dashed line shows phenomenological scaling, $< \delta y >= 0.58 y_p$, extracted from lower energy data [17–19]. The error bars at $y_p = 5.4$, the rapidity of the beam at $\sqrt{s_{NN}} = 200$, represents the difference between the two different fits. Clearly the constraint on the baryon-number ensures an accurate determination even though we did not measure up to the beam rapidity.

The lower energy data shown in figure 6 exhibit a linear relationship with y_p through SPS energies, $< \delta y >= 0.58 y_p$. This scaling is broken, however, at $\sqrt{s_{NN}} = 200$ GeV.

The energy loss can be determined using the total energy per net-baryon:

$$E = \frac{1}{N_{part}} \int_{-y_p}^{y_p} \langle m_T \rangle \cdot \cosh y \cdot \frac{dN_{B-\bar{B}}}{dy} \cdot dy. \tag{6}$$

resulting in 27 GeV which leads to an energy loss of 73 GeV out of the initial 100 GeV per participant, ie $\Delta E = 25.7$ TeV.

HIGH p_t SUPPRESSION

The Quark Gluon Plasma (QGP) is expected to be a dense medium. The search for signals indicating a dense medium began as soon as the first results from RHIC became available. One way to search for signals of a dense medium is to determine whether heavy ion collisions appear to reflect simple binary scaling of elementary nucleon-nucleon collisions or whether some other processes may be at work. A variable typically used to test nucleon-nucleon scaling is R_{AA}, defined as:

$$R_{AA} = \frac{1}{< N_{coll} >} \frac{d^2 N^{AuAu}/dp_t dy}{d^2 N^{pp}_{inel}/dp_t dy}. \tag{7}$$

where N_{coll} is the average number of binary collisions in the Au+Au event. R_{AA} is a measure of how much the nucleus-nucleus collisions deviate from simple nucleon-nucleon scaling. If, for example, R_{AA} has a value at or near unity, then nucleus-nucleus collisions are simply the superposition of simple binary scaling whereas if it is significantly different from unity, interesting phenomena may be observed. For example in reference [20] R_{AA} was observed to be larger than one. This was attributed to multiple scattering of partons in the initial stage of the reaction [20].

For our data, figure 7 shows R_{AA} as a function of p_t [21]. We observe in the top panel of figure 7 that for the 0-10% most central collisions, R_{AA} is significantly be-

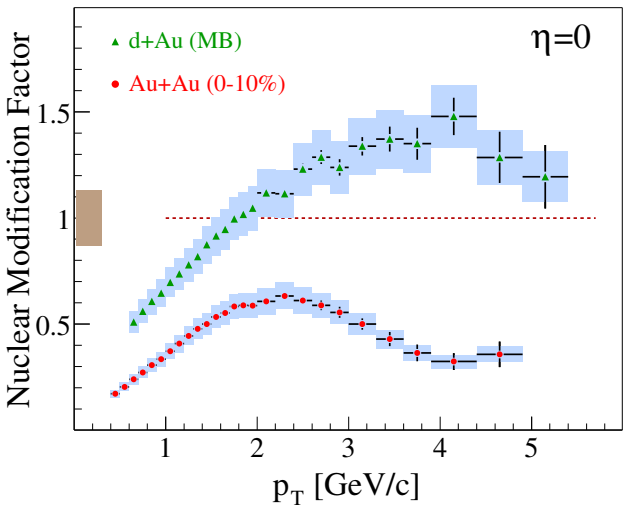

FIG. 8: Nuclear modification factor for minimum bias d + ^{197}Au collisions at $\sqrt{s_{NN}} = 200$ GeV(solid triangles) compared to central Au+Au collisions(solid circles).

low unity both at mid-rapidity (left panel) and at $\eta \sim 3.2$ (right panel). This could be indicative of a dense medium as higher p_t particles would be slowed and would show up at lower p_t. The center panels of figure 7 show the value of R_{AA} to be near one for $p_t >\sim 1.5$ possibly indicating a less dense medium for the less violent (more peripheral) collisions.

The bottom panels illustrate a possible signal for a dense medium using another related variable, R_{cp}. R_{cp} is is defined as:

$$R_{cp} = \frac{\frac{1}{<N_{coll}^{cent}>} N_{AB}^{cent}(p_t,\eta)}{\frac{1}{<N_{coll}^{perip}>} N_{AB}^{perip}(p_t,\eta)} \qquad (8)$$

It is based on the expectation that any nuclear modification in peripheral collisions is not significant. This is a reasonable assumption given the observation in the center panels for R_{AA} of the peripheral collisions.

This variable has the advantage of being independent of the results for the elementary reference, ie p+p. We see in the bottom panels that this variable is also significantly below unity consistent with R_{AA} in the top panel.

The interpretation of figure 7 as evidence of a dense medium produced in the most violent ^{197}Au + ^{197}Au collisions is dependent upon whether the results come from initial state or final state effects. To test this, BRAHMS (as well as the other three RHIC experiments) measured R_{dA} for d+^{197}Au at $\sqrt{s_{NN}} = 200$. The R_{dA} results from our experiment are shown as triangles in figure 8. We observe R_{dA} is significantly larger than one at $p_t > 2$ in contrast to R_{AA} from ^{197}Au + ^{197}Au (solid circles; same as left top panel of figure 7). This shows clearly and unambiguously that the R_{AA} for ^{197}Au + ^{197}Au at $\sqrt{s_{NN}} = 200$ results from final state effects and not initial state effects, providing convincing evidence for production of a heretofore unknown dense medium. The other three RHIC experiments reached similar conclusions [22–24] and these observations were undoubtedly the most exciting news in the relativistic heavy ion physics community in 2003.

HIGH p_t SUPPRESSION IN d+^{197}AU

We observed in figure 8 that R_{dA} for d+^{197}Au at $\sqrt{s_{NN}} = 200$ is significantly above one reflecting the long established Cronin effect [20]. Recall that R_{AA} for ^{197}Au + ^{197}Au shows suppression at $\eta \sim 2.2$. We have investigated the rapidity dependence of R_{dA} of d + ^{197}Au [25]. In figure 9 we show the rapidity dependence of R_{dA} from mid-rapidity (left panel) to $\eta \sim 3$ in the right panel. There is a clear evolution toward increasing suppression with rapidity. It has been proposed that this effect is related to the possible existence of the Color Glass Condensate (CGC) [26], a description of the ground state of the nuclei prior to collisions.

We also investigate the centrality dependence using the R_{cp} factors. Figure 10 shows the rapidity evolution for two sets of R_{cp}, central (0-10%) vs. peripheral (60-80%) (closed points) and semi-central (30-50%) vs. peripheral (60-80%) (open points). We see the enhancement at mid-rapidity consistent with R_{dA} in figure 9. This evolves toward suppression as the rapidity increases to $y \sim 3$. In addition, the central R_{cp} values show slightly more enhancement at mid-rapidity, roughly equal and near to one at $\eta = 1$. From that point the data exhibit more suppression as rapidity increases. This suggests that the suppression mechanism scales with the centrality of the collision.

Such a suppression has been qualitatively predicted by several authors [27–30] within the Color Glass Condensate picture. Recently a more quantitative framework for the CGC has been developed [31] by including realistic parton wave-functions along with valence quarks. In reference [31] the authors are able to obtain fairly quantitative agreement with our data, both in the magnitude of R_{dA} and in the magnitude and centrality dependence of R_{cp}.

PARTICLE RATIOS IN $p+p$ COLLISIONS

BRAHMS has also exploited its unique capabilities in the measurement of particle ratios in $p + p$ reactions. The understanding of the mechanism in $p + p$ is important as it forms the baseline for the investigations of the heavy ion systems. We have already discussed part of this importance in the earlier sections dealing with the high p_t suppression. We have also undertaken an analysis of particle ratios [32] over a large rapidity range. The

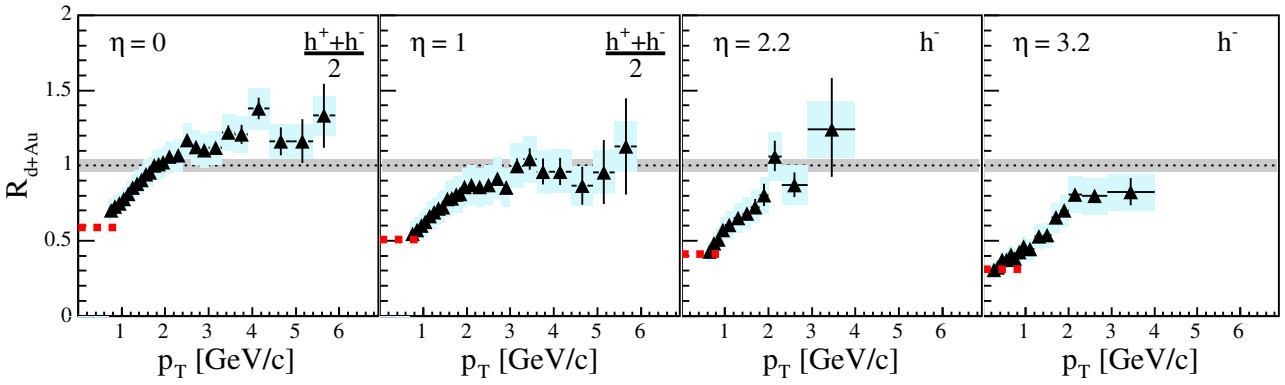

FIG. 9: Nuclear modification factors from d+^{197}Au collisions for charged hadrons for different pseudo-rapidities.

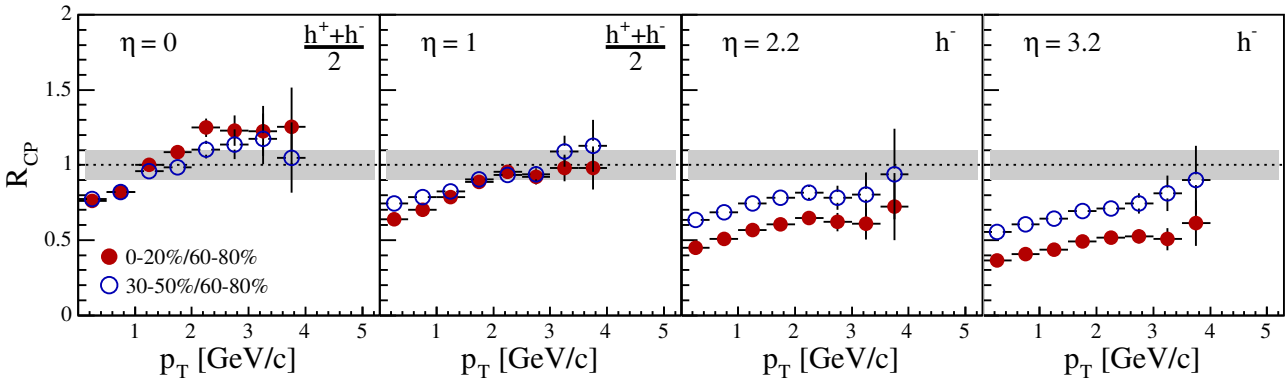

FIG. 10: R_{cp} for central (full points) and semi-central(open points) as a function of pseudo-rapidity from d+^{197}Au collisions.

left panels in figure 11 show the particle ratios for p+p collisions in a manner similar to that of figure 3. The top panel shows the ratios for pions, the center for the kaons and the bottom for the protons. Overlayed on the plots are open symbols which represent the ratios from Au + Au. In contrast to Au+Au, the $p+p$ pion ratios deviate from unity above $y \sim 2.5$. This can be attributed to isospin and charge conservation in the fragmentation region which is not seen in ^{197}Au+^{197}Au, where isospin equilibration is expected because of the large pion multiplicity.

Except for the pion ratios at $y >\sim 2.5$ the p+p ratios are nearly the same as the Au+Au ratios. This is very surprising in view of the significantly different dynamics expected in the two systems.

The solid curves show the predictions of the PYTHIA code [33]. The pion and kaon ratios are described by PYTHIA at mid-rapidity. In addition, the deviation of the pion ratios from unity at the higher rapidity is described by PYTHIA as well.

The proton ratios are not described by the PYTHIA calculation in any part of the rapidity range. To further investigate this observation, we also make comparisons to results of a calculation with the code HIJING/B [34]. The pion and kaon predictions of HIJING/B are very similar to those of PYTHIA. In contrast, the predicted proton ratios are somewhat lower and agree with the data rather well. This suggests that mechanisms other than quark di-quark breaking are necessary to transport the protons away from the beam rapidity. This is not to suggest that baryon junctions are the only mechanism to transport the protons from the beam rapidity, but that some additional mechanism is necessary.

The solid symbols in the right panels of figure 11 show the $p+p$ ratios at $\sqrt{s_{NN}} = 200$ GeV as a function of the difference of the rapidity from the beam rapidity. The open symbols show results from NA27 [35] at $\sqrt{s_{NN}} = 27.5$ GeV. The data are the same in the region of overlap suggesting the limiting fragmentation mechanism.

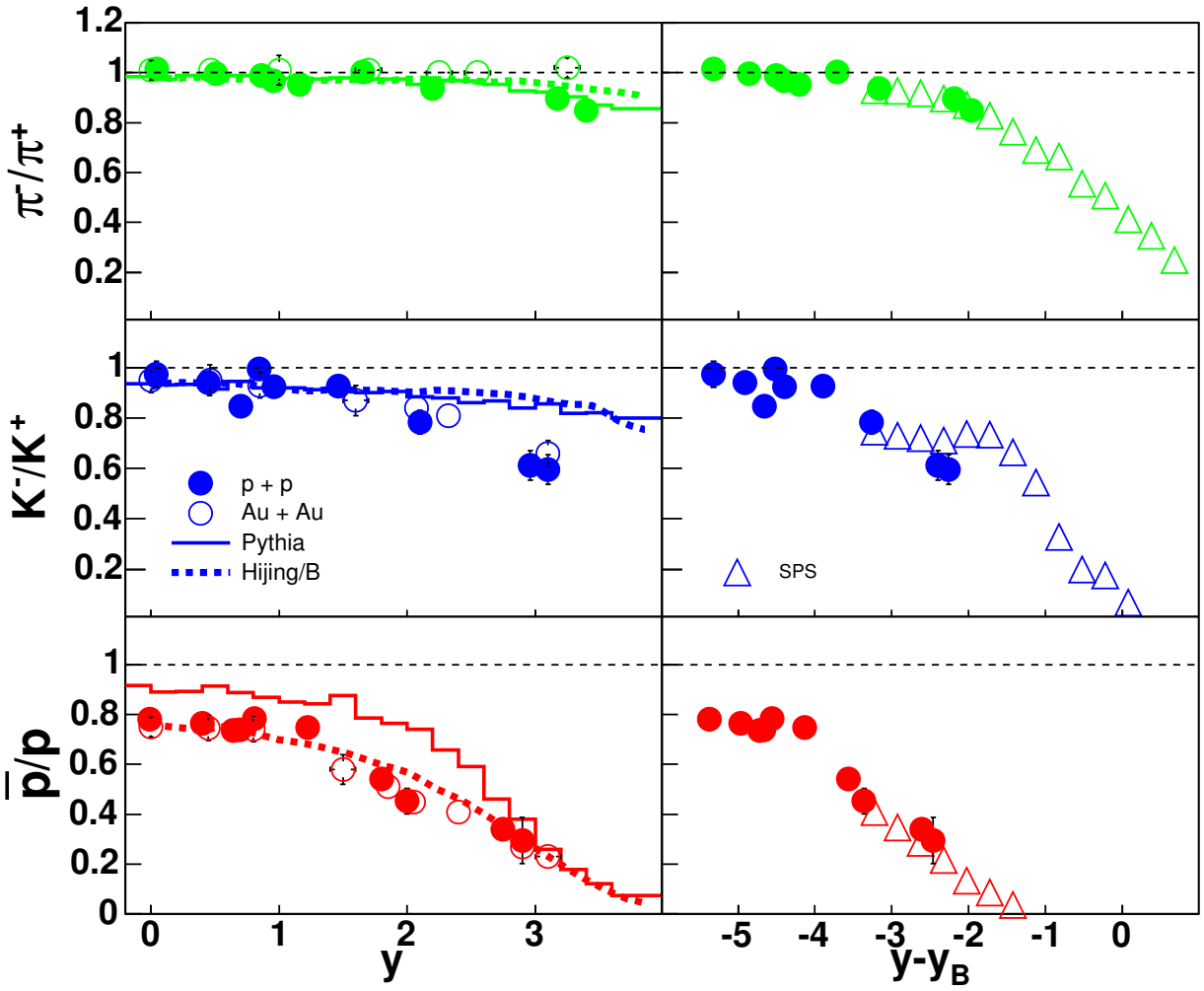

FIG. 11: Left: particle ratios as a function of rapidity. The closed symbols represent the ratios from p+p, the open symbols represent the ratios from Au+Au. The solid curve is the prediction of PYTHIA and the dashed curve is the prediction of HIJING/B. Right: Particle ratios as a function of the difference from the beam rapidity. The open symbols represent the p+p data at $\sqrt{s_{NN}}$ = 200 GeV and the open symbols represent the data at $\sqrt{s_{NN}}$ = 27.5 GeV [35]

SUMMARY

Measurements from BRAHMS have yielded a plethora of new results, especially in the forward region. These results are anchored by measurements of identified particle spectra over a large rapidity range, $0 < y < 3.2$. From this we obtained yields which led to a deduction of stopping and energy loss, as well as hints that we might be observing Landau flow. Measurements of baryon ratios show the creation of the largest ratio of anti-matter to matter yet observed. Correlations of K^-/K^+ to $\bar{p}/p$ show a seemingly universal relationship. From that we are able to estimate baryon-chemical potential as well as a limit on strangeness content. Studies of high p_t suppression in ^{197}Au + ^{197}Au at mid-rapidity yielded the observation of a new state of dense matter. Studies of high p_t suppression in d + ^{197}Au show the possible existence of the Color Glass Condensate, a description of the ground state of nuclei prior to collisions. Particle ratios in $p + p$ collisions at $\sqrt{s_{NN}}$ = 200 GeV show surprising similarities to the ratios from ^{197}Au + ^{197}Au. In addition, the data show evidence for limiting fragmentation when compared to lower energy data in $y - y_b$.

All of these conclusions depend upon the results at forward angles for their interpretation. There are many new data currently under analysis, notably for ^{197}Au + ^{197}Au at $\sqrt{s_{NN}}$ = 62 GeV, which also benefit from our broad measurement capability. In addition the next RHIC run with Cu+Cu will add results in an intermediate mass region to the already impressive results.

ACKNOWLEDGEMENTS

This work was supported by the United States Department of Energy under Grant # DE-FG03- 93ER40773, the Danish Natural Science Research Council, the Research Council of Norway, the Polish State Committee for Scientific Research (KBN) and the Romanian Ministry of Research.

---

* E-mail at:hagel@comp.tamu.edu

[1] M. Adamczyk *et al.*, BRAHMS Collaboration, Nucl. Instr. Meth. A **499** (2003) 437.
[2] N. Herrmann *et al.*, Ann. Rev. Nucl. Part. Sci. **49** (2000) 581.
[3] H. Satz, Rep. Prog. Phys. **63** (2000) 1511.
[4] I. G. Bearden *et al.*, Phys. Rev. Lett. **90** (2003) 102301.
[5] P. Braun-Munzinger *et al.*, Phys. Lett. **B518** (2000) 41.
[6] I. G. Bearden *et al.*, Phys. Rev. Lett. **87** (2001) 112305.
[7] L. Ahle *et al.*, E866 Collaboration, Phys. Rev. Lett. **81** (1998) 2560 and Phys. Rev. C **60** (1999) 044904.
[8] Y. Afanasiev *et al.*, NA49 Collaboration, nucl-ex/0205002; J. Bächler *et al.*, Nucl. Phys. **A661** (1999) 45.
[9] I. G. Bearden *et al.*, NA44 Collaboration, J. Phys. G, Nucl. Part. **23** (1997) 1865.
[10] J. Rafelski, Phys. Lett. **B262** (1991) 333.
[11] F. Becattini *et al.*, Phys. Rev. C **64** (2001) 24901.
[12] L. D. Landau, Izv. Akad. Nauk SSSR **17** (1953) 52.
[13] P. Carruthers *et al.*, Phys. Rev. D **8** (1973) 859.
[14] J. D. Bjorken, Phys. Rev. D **27** (1983) 140.
[15] B. B. Back *et al.*, PHOBOS Collaboration, nucl-ex/0301017.
[16] I. G. Bearden *et al.*, Phys. Rev. Lett **93** (2004) 102301.
[17] F. Videbaek and O. Hansen, Phys. Rev. C **52** (1995) 2684.
[18] B. Hong *et al.*, FOPI Collaboration, Phys. Rev. C **57** (1998) 244; **58** (1998) 603.
[19] B. B. Back *et al.*, E917 Collaboration, Phys. Rev. Lett. **86** (2001) 1970
[20] J. W. Cronin *et al.*, Phys. Rev. D **11** (1975) 3105.
[21] I. Arsene *et al.*, Phys. Rev. Lett. **91** (2003) 072305.
[22] B. B. Back *et al.*, Phys. Rev. Lett. **91** (2003) 072302.
[23] J. Adams *et al.*, Phys. Rev. Lett. **91** (2003) 072304.
[24] S. S. Adler *et al.*, Phys. Rev. Lett. **91** (2003) 072303.
[25] I Arsene *et al.*, nucl-ex/0403005, accepted for publication, PRL (2004).
[26] D. Kharzeev *et al.*, Phys Lett **B561** (2003) 93.
[27] A. Dumitru *et al.*, Phys. Lett. **B547** (2002) 15.
[28] J. Jalilian-Marian *et al.*, Phys. Lett. **B577** (2003) 54; A. Dumitru *et al.*, Phys. Rev. Lett **89** (2002) 022301.
[29] R. Baier *et al.*, Phys. Rev. D **68** (2003) 054009.
[30] D. Kharzeev *et al.*, Phys. Rev. D **68** (2003) 094013; D. Kharzeev *et al.*, Phys. Lett. **B561** (2003) 93.
[31] D. Kharzeev *et al.*, Phys. Lett. **B599** (2004) 23.
[32] I. G. Bearden *et al.*, nucl-ex/0409002, accepted for publication, PRB (2004).
[33] T. Sjostrand *et al.*, Comput. Phys. Commun. **135** (2001) 238.
[34] S. E. Vance *et al.*, Phys. Lett. **B443** (1998) 45.
[35] M. Aguilar-Benitez *et al.*, Z. Phys. **C50** (1991) 405.